DOI: https://doi.org/10.30795/jfootankle.2022.v16.1673

Original Article

Ankle syndesmotic instability assessment using a three-dimensional distance mapping algorithm: a cadaveric pilot WBCT study

Kevin Dibbern[1], Grayson Talaski[1], Eli Schmidt[1], Ryan Jasper[1], Vineel Mallavarapu[1], Matthew Jones[1], Hannah Steabral[1], Andrew Behrens[1], Kepler Alencar Mendes de Carvalho[1], Ki Chun Kim[1,3], Nacime Salomão Barbachan Mansur[1,2], César de César Netto[1]

1. Department of Orthopedics and Rehabilitation, Carver College of Medicine, University of Iowa, IA, USA.
2. Department of Orthopedics and Traumatology, Paulista School of Medicine. Federal University of Sao Paulo, São Paulo, SP, Brazil.
3. Department of Orthopedic Surgery, Seoul Medical Center, Jungnang-gu, Seoul, South Korea.

Abstract

Objective: This cadaveric pilot study was to develop a weight bearing computed tomography (WBCT) three-dimensional (3D) distance mapping algorithm that would allow for detection of syndesmotic instability.

Methods: Pilot study, two cadaveric specimens. Syndesmotic instability was induced by release of all syndesmotic ligaments through a conventional lateral ankle approach. WBCT imaging under simulated weight bearing was acquired before and after syndesmotic destabilization. Syndesmotic incisura and ankle gutter distances were assessed using a 3D distance mapping WBCT algorithm.

Results: We found increases in the overall mean syndesmotic distances in the injured syndesmosis when compared to pre-injury state, and color-coded distance maps allowed easy interpretation of the syndesmotic widening following ligament sectioning and destabilization of the syndesmotic joint.

Conclusion: The WBCT 3D distance mapping algorithm has the potential to allow detection of mild syndesmotic instability with a relatively ease of interpretation by using color-coded distance maps.

Level of Evidence V; Cadaveric Study.

Keywords: Joint instability; Orthopedic procedures; Syndesmosis; Tomography, x-ray computed; Weight-bearing.

Introduction

The importance of the distal tibiofibular syndesmotic ligaments in maintaining the overall stability of the ankle joint has been frequently emphasized in the literature. Ramsey and Hamilton[1], in their classic study, demonstrated that a minimal lateral displacement of one millimeter of the talus within the ankle mortise would lead to a decrease of 42% of the ankle contact area. This decrease in total contact area could cause an increase in the articular pressures and subsequent joint degradation. Because of that, diagnosing syndesmotic instability is paramount.

Study performed at the UIOWA Orthopedic Functional Imaging Research Laboratory (OFIRL). University of Iowa, Carver College of Medicine, Department of Orthopedics and Rehabilitation, Iowa City, IA, USA.

Correspondence: Grayson Talaski. Carver College of Medicine, Department of Orthopedics and Rehabilitation University of Iowa, 200, 52242-0000, Hawkins Dr. John PappaJohn Pavillion (JPP), Iowa City, IA, USA. **E-mail:** gtalaski@uiowa.edu. **Conflicts of interest: César de César Netto:** CurveBeam: Paid consultant; Stock or stock Options; Foot and Ankle International: Editorial or governing board; Editor in Chief Foot and Ankle Clinics; Nextremity: Paid consultant; Ossio: Paid consultant; Paragon 28: IP royalties, Paid consultant; Weightbearing CT; International Study Group: Board or committee member; Zimmer: Paid consultant. **Nacime Salomao Barbachan Mansur:** Brazilian Foot and Ankle Society: Board or committee member; American Orthopaedic Foot and Ankle Society: Board or committee member. **Source of funding:** none. **Date received:** December 9, 2022. **Date accepted:** December 11, 2022. **Online:** December 20, 2022.

How to cite this article: Dibbern K, Talaski G, Schmidt E, Jasper R, Mallavarapu V, Jones M, et al. Ankle syndesmotic instability assessment using a three-dimensional distance mapping algorithm: a cadaveric pilot WBCT study. J Foot Ankle. 2022;16(3):190-4.

Weight bearing computed tomography (WBCT) has emerged as a promising diagnostic tool that can assess the ankle joint under physiological weight-bearing load, potentially allowing detection of these small deviations of an unstable syndesmosis[2-5]. This weight load in isolation has been shown to not induce enough stress to reliably demonstrate syndesmotic instability[6,7], with a better diagnostic accuracy being observed when an external rotational torque is applied in combination[8,9]. This imaging modality also allows three-dimensional (3D) segmentation of the ankle bones and highly accurate assessments of the syndesmotic area and of volumetric measurements[10-13], as well as 3D distance mapping of the entire relationship between the talus, fibula, and tibia[14-16].

With that in mind, the overall objective of this cadaveric pilot study was to develop a WBCT 3D distance mapping algorithm that would allow for detection of mild syndesmotic instability in the absence of external rotation torque. The aim of this cadaveric pilot study is to describe the 3D WBCT Distance Mapping methodology utilized to detect syndesmotic instability.

Methods

In this cadaveric experimental pilot study, a total of two through-knee specimens were utilized. No prior surgical procedures or fractures were found, by means of fluoroscopic assessment. University Ethics Committee approved this research under the number 202006176 in accordance with the Declaration of Helsinki.

Specimen preparation and external frame

The proximal aspect of the through-knee specimens was prepared by detaching the surrounding soft tissue, with care to avoid destabilizing the proximal tibiofibular joint. The proximal tibia was then potted in a square block using polymethylmethacrylate bone cement. The cemented block was utilized to fix the specimen vertically and in a plantigrade fashion into an external radiolucent frame that was previously utilized in the literature to allow for simulated weight bearing[17]. Weight bearing was simulated by introducing 36.3 kilograms (356N) of vertical load into the specimen frame construct (Figure 1).

Simulated weight-bearing CT imaging

The radiolucent frame with the specimen under simulated weight-bearing was place in a WBCT scan machine (HiRise, Curvebeam®), and images of the foot and ankle were acquired under a metal artifact reduction algorithm. Each specimen underwent a total of three WBCT images with simulated weight bearing in the external frame. The initial imaging was acquired as a baseline normal scan with intact syndesmotic ligaments performed after the specimen was thawed. The second set of WBCT images was acquired after the syndesmotic ligaments were surgically sectioned.

Surgical procedures

Surgical procedures were all performed by a single fellowship-trained orthopedic foot and ankle surgeon with more than ten years of experience. All syndesmotic ligaments were released. The surgical sectioning of the syndesmotic ligaments was performed through a direct lateral approach to the distal fibula. The anteroinferior tibiofibular ligament (AITFL) and the interosseus ligaments were sectioned under direct visualization of the anterior aspect of the syndesmosis. The posteroinferior tibiofibular ligament (PITFL) was sectioned under direct visualization posteriorly, by retracting the peroneal tendons and giving access to the posterior aspect of the syndesmosis. The superior peroneal retinaculum and deltoid ligament complex were kept intact.

3D distance mapping

Creation of distance maps began with a semi-automated segmentation of the tibia, talus, and fibula using a commercially available software package (Bonelogic, Disior™). Models were verified and finalized by an expert with more than 9 years of image segmentation experience to remove any imperfections. Thousands of distance measurements were then automatically made based on a previously published protocol[18] (Figure 2) and were performed along the entire tibiofibular interface and additionally included the gutters of the ankle joint.

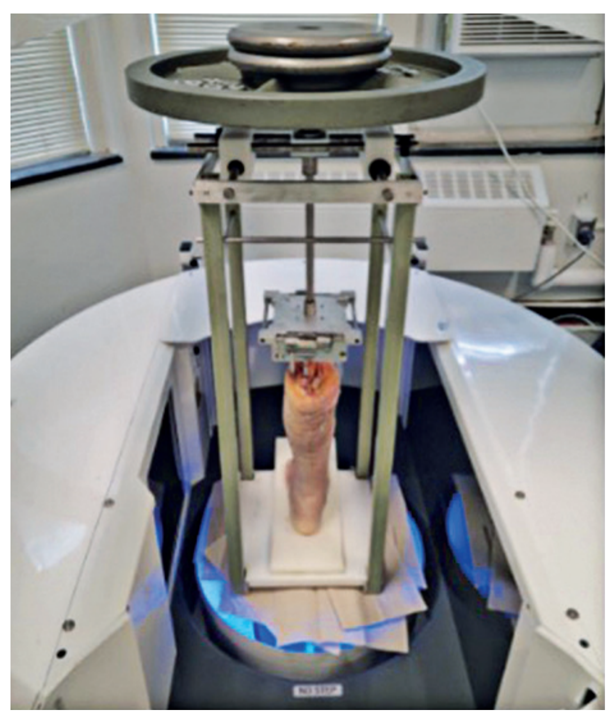

Figure 1. WBCT scanner and radiolucent external frame, which holds the leg in the simulated weight-bearing position.

Measurements performed in articular areas were defined as the distance along the normal direction of vectors projected from the tibial subchondral surface to the opposing surfaces of the talus or distal fibula, as previously described[19,20]. Distances in the syndesmosis were defined along the averaged normal direction between the fibula and tibia.

Color-Coded maps were then created to facilitate the interpretation of distance maps results. For each one of the WBCT scans (before and after syndesmotic ligament sectioning), the distances between the tibia and fibula were color-coded with small distances (0-5 mm) ranging from dark to light blue, and larger distances (6-10 mm) ranging from green to dark yellow and then light yellow. The comparative assessment between pre-injury to post-syndesmotic ligament sectioning utilized then a different set of color-coded maps (post-injury minus pre-injury state). When the post-injury unstable state demonstrated relative widening of the syndesmotic space when compared to the pre-injury state, red color was utilized to depict widening. White colored maps demonstrated similar syndesmotic distances before and after syndesmotic destabilization, and blue color depicted decreased and closer relative distances between the tibia and the fibula when comparing post and pre syndesmotic injury.

Volumetric and area analyses

Automated volumetric and area measurements of the distal tibiofibular syndesmosis at 1cm, 3cm, and 5cm from the tibiotalar joint (apex of the distal tibia articular dome) were performed (Figure 3).

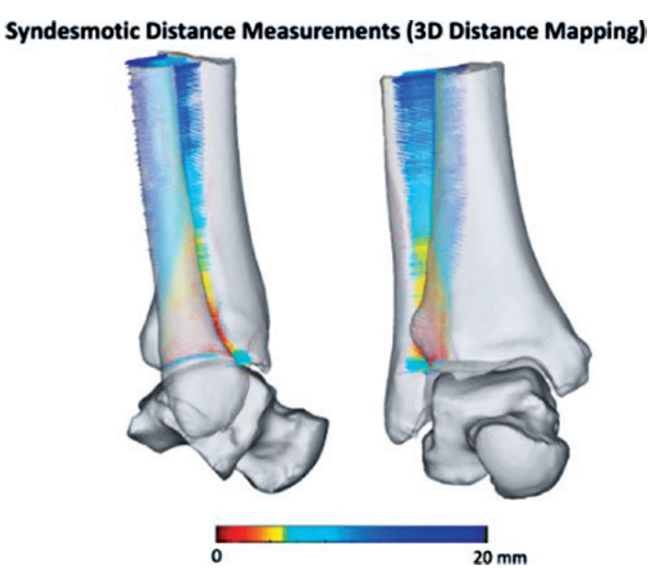

Figure 2. Three-Dimensional distance measurements (distance mapping) of the tibiofibular relationships.

Results

We found overall increases in the mean syndesmotic distances between the distal tibia an fibula in the injured unstable state when compared to the native pre-injury state. Qualitatively, these changes were visually apparent in comparison distance maps (Figure 4), with diffuse red colors

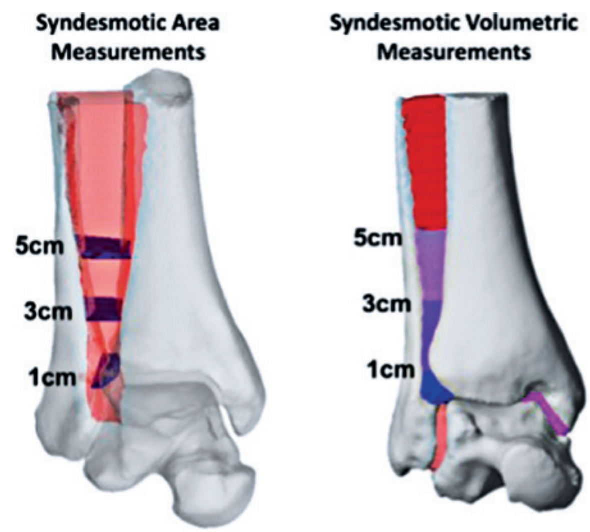

Figure 3. Three-Dimensional graphical representation of area (left) and volumetric (right) measurements of syndesmotic relationship at 1, 3, 5cm proximally to the ankle joint line.

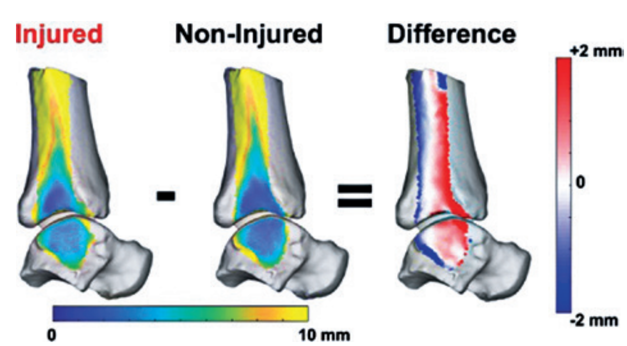

Figure 4. Distance mapping of the injured state (left), uninjured state (middle), and the difference between the injured and uninjured (right). Relative widening in the injured condition (red), narrowing (blue) and no relative change (white). Small distances (0-5mm) ranging from dark to light blue, and larger distances (6-10mm) ranging from green to dark yellow and then light yellow (first two images). In the comparative assessment between post--injury minus pre-injury state (third image), red color was utilized to depict widening, white color demonstrated similar syndesmotic distances, and blue color depicted decreased and closer relative distances between the tibia and the fibula when comparing post and pre syndesmotic injury.

in the comparative color-coded distance maps, particularly in the anterior aspect of the tibiofibular syndesmosis and lateral ankle gutter.

Discussion

This cadaveric pilot study aimed to assess the capability of a WBCT 3D distance mapping algorithm in identifying syndesmotic injury and instability. The 3D WBCT distance mapping algorithm demonstrated promising diagnostic capability even in the absence of external rotation torque applied in the cadaveric specimen, shining light in the possibility of development of a non-invasive diagnostic tool to detect mild syndesmotic instability. To the author's knowledge, this was the first pilot study to utilize 3D distance mapping in the assessment of syndesmotic Instability.

The use of 3D WBCT distance mapping is an emerging technique with the intrinsic potential of assessing bone interaction in a wide range of orthopedic conditions[14,15,21]. Dibbern et al.[20] used the technology to exhibit differences in peritalar subluxation in patients with progressive collapsing foot deformity and controls (decreased middle facet coverage: 46.6%, $p<0.001$, increase sinus tarsi coverage: 98.0%, $p<0.007$). When evaluating cavovarus deformities, Lintz et al.[15] used WBCT distance mapping to objectively represent several positional changes in the diseased population, such as the ankle, subtalar, midtarsal, and tarsometatarsal joints. Fibular malpositioning in subtle syndesmotic instability can be in the range of the tenth of the millimeters, making it impossible for conventional, manual, and isolated measurements to make accurate diagnosis[3,8,22]. Given this, and considering all the challenges of a reliable clinical diagnosis, this new technology can hopefully provide ground-breaking and accurate assessment of these extremely challenging and unforgiving injury[23,24]. Additional full study with larger number of cadaveric specimens as well as clinical applicability of this 3D WBCT distance mapping algorithm will follow.

Conclusion

In this cadaveric pilot study, we described a novel 3D WBCT distance mapping protocol to detect the relative positioning of the distal fibula and tibia, aiming to develop an accurate diagnostic tool to detect subtle syndesmotic instability, in the absence of external ration torque application. The color-coded 3D distance maps acquired allowed for a relatively simple interpretation of syndesmotic distances, particularly in the comparative pre- and post-injury analysis, that could allow for detection of subtle syndesmotic instability by means of visual interpretation of the distance maps. This technology could be applied to a comparison between injured versus contralateral control side in a clinical scenario of potential subtle syndesmotic instability. Additional large scale cadaveric and clinical studies are needed to establish the role of WBCT 3D distance mapping in the diagnosis and management of ankle syndesmotic instability.

Authors' contributions: Each author contributed individually and significantly to the development of this article: KD *(https://orcid.org/0000-0002-8061-4453), and GT *(https://orcid.org/0000-0002-0018-6410) Conceived and planned the activities that led to the study, interpreted the results of the study, participated in the review process and approved the final version; ES *(https://orchid.org/0000-0002-6922-5238) Data collection and interpreted the results of the study, and approved the final version; VM *(https://orcid.org/0000-0002-8612-5941), and RJ *(https://orcid.org/0000-0003-3448-1300), and MJ *(https://orcid.org/0000-0003-0773-7286), and HS *(https://orcid.org/0000-0003-2664-0762), and AB *(https://orcid.org/ 0000-0002-4588-9291), and KCK *(https://orcid.org/0000-0002-3731-8448) Data collection and interpreted the results of the study; KAMC *(https://orcid.org/0000-0003-1082-6490) Interpreted the results of the study, participated in the review process and approved the final version; NSBM *(https://orcid.org/0000-0003-1067-727X) Interpreted the results of the study and approved the final version; CCN *(https://orcid.org/0000-0001-6037-0685) Interpreted the results of the study and approved the final version. All authors read and approved the final manuscript. *ORCID (Open Researcher and Contributor ID) .

References

1. Ramsey PL, Hamilton W. Changes in tibiotalar area of contact caused by lateral talar shift. J Bone Joint Surg Am. 1976;58(3):356-7.
2. Barg A, Bailey T, Richter M, et al. Weightbearing computed tomography of the foot and ankle: emerging technology topical review. Foot Ankle Int. 2018;39(3):376-86.
3. de Cesar Netto C. CORR Insights®: Can Weightbearing Cone-beam CT Reliably Differentiate Between Stable and Unstable Syndesmotic Ankle Injuries? A Systematic Review and Meta-Analysis. Clin Orthop Relat Res. 2022;480(8):1563-5.
4. Lintz F, de Cesar Netto C, Barg A, Burssens A, Richter M; Weight Bearing CT International Study Group. Weight-bearing cone beam CT scans in the foot and ankle. EFORT Open Rev. 2018;3(5):278-86.
5. Raheman FJ, Rojoa DM, Hallet C, Yaghmour KM, Jeyaparam S, Ahluwalia RS, et al. Can Weightbearing Cone-beam CT Reliably Differentiate Between Stable and Unstable Syndesmotic Ankle Injuries? A Systematic Review and Meta-analysis. Clin Orthop Relat Res. 2022;480(8):1547-62.
6. Krähenbühl N, Bailey TL, Weinberg MW, Davidson NP, Hintermann B, Presson AP, et al. Is load application necessary when using computed tomography scans to diagnose syndesmotic injuries? A cadaver study. Foot Ankle Surg. 2020;26(2):198-204.
7. Shakoor D, Osgood GM, Brehler M, Zbijewski WB, de Cesar Netto C, Shafiq B, et al. Cone-beam CT measurements of distal tibio-fibular syndesmosis in asymptomatic uninjured ankles: does weight-bearing matter? Skeletal Radiol. 2019;48(4):583-94.
8. Burssens A, Krahenbuhl N, Weinberg MM, Lenz AL, Saltzman CL,

Barg A. Comparison of external torque to axial loading in detecting 3-dimensional displacement of syndesmotic ankle injuries. Foot Ankle Int 2020;41(10):1256-68.

9. Krähenbühl N, Bailey TL, Weinberg MW, Davidson NP, Hintermann B, Presson AP, et al. Impact of Torque on Assessment of Syndesmotic Injuries Using Weightbearing Computed Tomography Scans. Foot Ankle Int. 2019;40(6):710-9.
10. Ashkani Esfahani S, Bhimani R, Lubberts B, Kerkhoffs GM, Waryasz G, DiGiovanni CW, et al. Volume measurements on weightbearing computed tomography can detect subtle syndesmotic instability. J Orthop Res. 2022;40(2):460-7.
11. Auch E, Barbachan Mansur NS, Alexandre Alves T, Cychosz C, Lintz F, Godoy-Santos AL, et al. Distal tibiofibular syndesmotic widening in progressive collapsing foot deformity. Foot Ankle Int. 2021;42(6):768-75.
12. Bhimani R, Ashkani-Esfahani S, Lubberts B, Guss D, Hagemeijer NC, Waryasz G, et al. Utility of Volumetric Measurement via Weight-Bearing Computed Tomography Scan to Diagnose Syndesmotic Instability. Foot Ankle Int. 2020;41(7):859-65.
13. Hagemeijer NC, Chang SH, Abdelaziz ME, Casey JC, Waryasz GR, Guss D, et al. Range of Normal and Abnormal Syndesmotic Measurements Using Weightbearing CT. Foot Ankle Int. 2019; 40(12):1430-7.
14. Bernasconi A, De Cesar Netto C, Siegler S, Jepsen M, Lintz F; International Weight-Bearing CT Society. Weightbearing CT assessment of foot and ankle joints in Pes Planovalgus using distance mapping. Foot Ankle Surg. 2022;28(6):775-84.
15. Lintz F, Jepsen M, De Cesar Netto C, Bernasconi A, Ruiz M, Siegler S; International Weight-Bearing CT Society. Distance mapping of the foot and ankle joints using weightbearing CT: The cavovarus configuration. Foot Ankle Surg. 2021;27(4):412-20.
16. Siegler S, Konow T, Belvedere C, Ensini A, Kulkarni R, Leardini A. Analysis of surface-to-surface distance mapping during three-dimensional motion at the ankle and subtalar joints. J Biomech. 2018;76:204-11.
17. Lalevée M, Dibbern K, Barbachan Mansur NS, Walt J, Lee HY, Coillard JY, et al. Impact of First Metatarsal Hyperpronation on First Ray Alignment: A Study in Cadavers. Clin Orthop Relat Res. 2022;480(10):2029-40.
18. Goetz JE, Rungprai C, Rudert MJ, Warth LC, Phisitkul P. Screw fixation of the syndesmosis alters joint contact characteristics in an axially loaded cadaveric model. Foot Ankle Surg. 2019;25(5):594-600.
19. Day MA, Ho M, Dibbern K, Rao K, An Q, Anderson DD, et al. Correlation of 3D Joint Space Width From Weightbearing CT With Outcomes After Intra-articular Calcaneal Fracture. Foot Ankle Int. 2020;41(9):1106-16.
20. Dibbern KN, Li S, Vivtcharenko V, Auch E, Lintz F, Ellis SJ, et al. Three-Dimensional Distance and Coverage Maps in the Assessment of Peritalar Subluxation in Progressive Collapsing Foot Deformity. Foot Ankle Int. 2021;42(6):757-67.
21. Gardner MJ, Demetrakopoulos D, Briggs SM, Helfet DL, Lorich DG. Malreduction of the tibiofibular syndesmosis in ankle fractures. Foot Ankle Int. 2006;27(10):788-92.
22. Kubik JF, Rollick NC, Bear J, Diamond O, Nguyen JT, Kleeblad LJ, et al. Assessment of malreduction standards for the syndesmosis in bilateral CT scans of uninjured ankles. Bone Joint J. 2021; 103-B(1):178-83.
23. Corte-Real N, Caetano J. Ankle and syndesmosis instability: consensus and controversies. EFORT Open Rev. 2021;6(6):420-31.
24. Tourné Y, Molinier F, Andrieu M, Porta J, Barbier G. Diagnosis and treatment of tibiofibular syndesmosis lesions. Orthop Traumatol Surg Res. 2019;105(8S):S275-S86.